Visualising the roots of quadratic equations with complex coefficients

Nicholas S. Bardell
QuEST Global Engineering
<nick.bardell@quest-global.com>

Introduction

This paper is a natural extension of the root visualisation techniques first presented by Bardell (2012) for quadratic equations with real coefficients. Consideration is now given to the familiar quadratic equation $y = ax^2 + bx + c$ in which the coefficients a, b, c are generally complex, as shown explicitly in Equation (1) with the usual notation.

$$y = (a_R + ia_I)x^2 + (b_R + ib_I)x + (c_R + ic_I) \tag{1}$$

The roots are most easily found from the 'standard' quadratic equation formula, suitably modified to account for the complex coefficients thus:

$$x = \frac{-(b_R + ib_I) \pm \sqrt{(b_R + ib_I)^2 - 4(a_R + ia_I)(c_R + ic_I)}}{2(a_R + ia_I)} \tag{2}$$

A routine application of Equation (2) will furnish the desired roots, and for most students this is usually the final step in a given analysis. However, there are many rich nuggets of information to be mined from a fuller consideration of Equations (1) and (2), with the *pièce de résistance* being an ability to somehow visualise the location and nature of the roots.

Surprisingly little has been written about this topic. Hardy (2008, pp. 94–95) finds the solution for the roots by dividing Equation (1) through by the $(a_R + ia_I)$ term, effectively forcing the leading coefficient to be monic and thus losing the general condition that all coefficients are arbitrary complex numbers. His solutions are thus non-generic, and some of the conditions he puts forward for the type of roots that result from a given set of complex coefficients are therefore of limited value. McCarthy (n.d.) has also noted these shortcomings. In response he has produced a highly insightful article about the most general form of a quadratic equation with generally complex coefficients, as shown in Equation (1), and therein derives various criteria that can be applied to the complex coefficients in order to predict particular

types of roots. His solutions are totally generic and accord with the current work; all of his various root criteria are tried, tested, and proved herein.

A reasonable starting point would focus on plotting the curve represented by Equation (1). This is more difficult than it looks, and a simple x–y plot can only be found by separating the real and imaginary components of y and presenting them both on the same set of axes. However, such a plot is hard to interpret and in general does not reveal any information about the location or the nature of the roots. It is a lamentable fact that few mathematics text books get even this far, and the remarkable dearth of information on this particular topic has been noted by Hardy (2008, pp. 94–95) and McCarthy (n. d.). By way of illustration, consider the following equation:

$$y = (1-i)x^2 + (-2+6i)x + (3-2i) \tag{3}$$

The real and imaginary parts are plotted separately over the range $-4 \le x \le 6$ as shown in Figure 1.

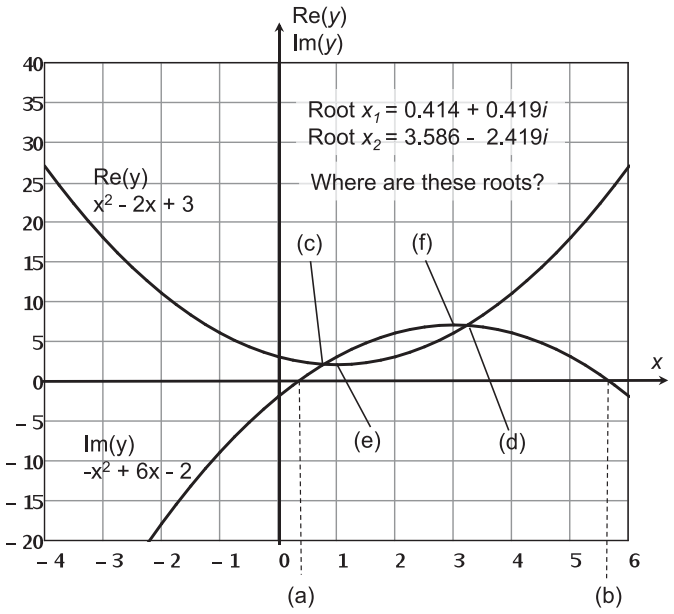

Figure 1. Plot of the real and imaginary parts of Equation (3).

Although the curves for $Re(y)$ and $Im(y)$ may intersect each other and/or the x-axis once, twice, or not at all, there is no great significance to any of these intersections. From Equation (2) the roots are determined as: $x_1 = 0.414 + 0.419i$ and $x_2 = 3.586 - 2.419i$. From Figure 1, the $Im(y)$ curve crosses the x-axis at points (a) $x = 0.354$ and (b) $x = 5.646$; the common intersection between the $Re(y)$ and $Im(y)$ curves occurs at points (c) $x = 0.775$ and (d) $x = 3.225$; and the vertices of either curve are located at points (e) $x = 1$ and (f) $x = 3$. None of these points (a) to (f) corresponds to the real or imaginary part of either root. Such observations beg the questions: Where are the roots located, why does the x–y plot give no hint of their nature, and how can we visualise things more clearly?

The aim of this paper is to answer these fundamental questions. The explanations offered will be of most interest to those teaching and studying a Mathematics Specialism (ACARA, n.d., Unit 3) such as the Victorian VCE (Specialist Mathematics, 2010), HSC in NSW (Mathematics Extension in NSW, 1997) or Queensland QCE (Mathematics C, 2009). Some of the stated aims of Specialist Mathematics (ACARA, n.d., Rationale) are to develop students'

- "understanding of concepts and techniques drawn from complex numbers",
- "ability to solve applied problems using concepts and techniques drawn from complex numbers" and
- "capacity to choose and use technology appropriately".

Whilst the basics of these topics may be thoroughly covered in various textbooks, real-world applications and visualisations of these concepts are not —this paper helps answer these needs.

Theory: Complex generalisation

Since the roots resulting from Equation (2) can be complex, this implies that the values assigned to x in Equation (1) do not have to be limited to the set of real numbers but rather could—and possibly should—include complex values. Whilst this is implicitly obvious, since no restriction was ever placed on x or y at the outset, it is rarely presented as an explicit proposition. Perhaps one reason why this is seldom considered is simply one of expedience —constructing a plot using generally complex values of x is not for the faint-hearted! Nevertheless, if this line of reasoning is pursued, and x is allowed to take a generally complex value $G + iH$, in which i is the complex number $\sqrt{-1}$, then substituting this into Equation (1) yields:

$$y = (a_R + ia_I)(G + iH)^2 + (b_R + ib_I)(G + iH) + (c_R + ic_I) \tag{4a}$$

Equation (4a) can be expanded and simplified to

$$\begin{aligned} y = {} & a_R G^2 - a_R H^2 - 2a_I GH + b_R G - b_I H + c_R \\ & + i(2a_R GH + a_I G^2 - a_I H^2 + b_R H + b_I G + c_I) \end{aligned} \tag{4b}$$

Since y must also be generally complex, of the form $A + iB$, then it is possible to equate the real (Re) and imaginary (Im) parts of both sides of Equation (4b).

Equating Re parts: $A = a_R G^2 - a_R H^2 - 2a_I GH + b_R G - b_I H + c_R$ (5)

Equating Im parts: $B = 2a_R GH + a_I G^2 - a_I H^2 + b_R H + b_I G + c_I$ (6)

Equations (5) and (6) represent three-dimensional surfaces describing the generalised complex form of Equation (1). It is noted that when $H = 0$, i.e., a section taken through either surface to reveal the real GA or GB plane, that the equations $A = a_R G^2 + b_R G + c_R$ and $B = a_I G^2 + b_I G + c_I$ are obtained, and

the trace of each of these curves is nothing more than the original Equation (1) split into its real and imaginary parts. It is now becoming evident that the x–y plane shown in Figure 1 is simply a two-dimensional 'slice' of a more general three-dimensional solution space. This latter three-dimensional representation contains all the information necessary to reveal the nature of the roots given by Equation (2) and will be used to explain why they can occur in any general combination.

The surface A for Re(y)

The expression for $Re(y)$ shown in Equation (5) is a quadric surface that can be identified and classified by reducing it to its simplest (canonical) form by translation and rotation of axes. See Bardell (2012, Appendix A), for further details, and the procedure for determining the expressions for m, n, p and β. Thus:

$$G' = G - m \tag{7a}$$

$$H' = H - n \tag{7b}$$

$$Z_A = A - p \tag{7c}$$

where

$$m = \frac{-(b_R a_R + b_I a_I)}{2(a_R^2 + a_I^2)} \tag{7d}$$

$$n = \frac{-(b_I a_R - b_R a_I)}{2(a_R^2 + a_I^2)} \tag{7e}$$

$$p = \frac{-b_R{}^2 a_R - 2b_R b_I a_I + b_I^2 a_R + 4a_R^2 c_R + 4a_I^2 c_R}{4(a_R^2 + a_I^2)} \tag{7f}$$

followed by a counter-clockwise rotation in the plane of the newly translated $G'H'$ axes about a normal through the local origin by an amount β_A where

$$\tan\beta_A = \frac{a_R - \sqrt{a_R{}^2 + a_I{}^2}}{a_I} \tag{7g}$$

This coordinate transformation renders Equation (5) in the form,

$$Z_A = \sqrt{a_R{}^2 + a_I{}^2} X_A{}^2 - \sqrt{a_R{}^2 + a_I{}^2} Y_A{}^2 \tag{8}$$

which is readily classified as a hyperbolic paraboloid with a vertex centred at (m, n, p). This surface can easily be constructed over a range of G, H values for a specific quadratic equation with complex coefficients (see Bardell (2012, pp. 8–9). The following observations follow:

- Only a_I, the imaginary part of the coefficient of the x^2 term, causes the rotation of the principal planes of the surface A. If $a_I = 0$ then the orientation of the principal planes will align with the $G'H'$-axes. (This result follows from Equation (7g), despite it appearing to become indeterminate on account of the right hand side becoming $0/0$. However, a single application of L'Hôpital's rule confirms that in the limit as $a_I \to 0$, the expression for the right hand side also tends to zero, and hence $\beta_A = 0$).

- The altitude p of the local $G'H'$ origin above the GH plane is independent of c_I but dependent on all the other coefficients.
- When the imaginary components of all the coefficients are zero, familiar results for the real coefficient case are recovered, as expected; see Bardell (2012) for a comparison.

The surface B for Im(y)

The expression for $Im(y)$, as shown in Equation (6), is also that of a general quadric surface, with many similarities to surface A. Once again, by adopting exactly the same approach to transform and rotate the GHB axes, this equation can also be reduced to its simplest (canonical) form thus:

$$G' = G - q \tag{9a}$$

$$H' = H - r \tag{9b}$$

$$Z_B = B - s \tag{9c}$$

where

$$q = \frac{-(b_R a_R + b_I a_I)}{2(a_R^2 + a_I^2)} \tag{9d}$$

$$r = \frac{-(b_I a_R - b_R a_I)}{2(a_R^2 + a_I^2)} \tag{9e}$$

$$s = \frac{-{b_I}^2 a_I - 2b_R b_I a_R + b_R^2 a_I + 4a_R^2 c_I + 4a_I^2 c_I}{4(a_R^2 + a_I^2)} \tag{9f}$$

followed by a counter-clockwise rotation in the plane of the newly translated $G'H'$ axes about a normal through the local origin by an amount β_B where

$$\tan\beta_B = \frac{-a_I + \sqrt{{a_R}^2 + {a_I}^2}}{a_R} \tag{9g}$$

This coordinate transformation renders Equation (6) in the form,

$$Z_B = \sqrt{{a_R}^2 + {a_I}^2}\,{X_B}^2 - \sqrt{{a_R}^2 + {a_I}^2}\,{Y_B}^2 \tag{10}$$

which again is readily classified as a hyperbolic paraboloid with a vertex centred at (q, r, s). This surface can also be constructed without difficulty; it is identical in form to that for A, (as confirmed by comparing Equations (8) and (10)) but differs in terms of its orientation—note the subtle difference between Equations (7g) and (9g)—and the altitude of its vertex origin above the GH-plane. The following observations follow:

- Only a_I, the imaginary part of the coefficient of the x^2 term, causes the rotation of the principal plane $X_B Z_B$ of the surface. If $a_I = 0$ then $\tan\beta_B = 1$ (from Equation (9g)) and the principal planes are rotated by $\pi/4$ counter-clockwise about a normal through the local $G'H'$ origin, as found by Bardell (2012) for the case with only purely real coefficients.
- The altitude s of the local $G'H'$ origin above the GH-plane is independent of c_R but dependent on all the other coefficients.

- When the imaginary components of all the coefficients are zero, the results for the real coefficient case are recovered, as expected; see Bardell (2012) for details.

The relation between the surfaces A and B

Both these surfaces share a common origin projected on to the horizontal *GH*-plane, since $m = q$ and $n = r$ as shown by Equations (7d), (9d) and (7e), (9e). Incidentally, these terms ((m, n) or (q, r)) may be verified to be the real and imaginary parts respectively of the first part of Equation (2), namely

$$\frac{-(b_R + ib_I)}{2(a_R + ia_I)} \tag{11}$$

rendered as a single complex number. This locates the common local $G'H'$ origin of both surfaces when viewed in the *GH*-plane. Note that in general, because both $m, q \neq 0$ and $n, r \neq 0$, the local origin of each surface no longer lies at a single point $(-b/2a)$ on the *G*-axis as it does for a quadratic equation with only real coefficients; indeed, it is now displaced away from the *GH* origin altogether such that it no longer lies in the *GA* plane, and it can vary in altitude. This is why a simple x–y plot of both $Re(y)$ and $Im(y)$, as shown in Figure 1, is unlikely to reveal the whereabouts of the roots, since a section taken at $H = 0$ will not, in general, pass through the common local $G'H'$ origin as it does in the case of real coefficients. Note also that the vertical location of each surface's origin—whether above or below the *GH*-plane—differs by an amount $(p - s)$. The terms p (see Equation (7f)) and s (see Equation (9f)) may also be verified as the real and imaginary parts of

$$\frac{-[(b_R + ib_I)^2 - 4(a_R + ia_I)(c_R + ic_I)]}{4(a_R + ia_I)} \tag{12}$$

which is just the term $-\Delta/4a$ generalised to its complex form; see Bardell (2012, Section 3.4) for further details. Here, the discriminant Δ takes the form $\Delta = (b_R + ib_I)^2 - 4(a_R + ia_I)(c_R + ic_I)$. It is important to note that the origin of the surface *B* is no longer coincident with the *GH*-plane, i.e., $s \neq 0$. It is for this reason that the $G'H'$ axes are shown projected on the zero plane in the plots that follow.

Although both *A* and *B* are now rotated relative to the *GH* axes, the orientation of the principal plane X_BZ_B of the surface *B* is always rotated counter-clockwise by a constant angle $\pi/4$ relative to the principal plane X_AZ_A of the surface *A* regardless of the values of the participating coefficients. This result follows immediately from the well-known tangent relationship

$$\tan(\beta_B - \beta_A) = \frac{\tan(\beta_B) - \tan(\beta_A)}{1 + \tan(\beta_B)\tan(\beta_A)} \tag{13}$$

which, upon substitution of the expressions for $\tan(\beta_A)$ from Equation (7g) and $\tan(\beta_B)$ from Equation (9g), reduces to

$$\tan(\beta_B - \beta_A) = 1 \tag{14a}$$

i.e.,

$$\beta_B - \beta_A = \frac{\pi}{4} \tag{14b}$$

Both surfaces are hence 'locked' together in terms of their rotational relationship, and the *GH* coordinates of their origin; however, they are 'free' to rotate in unison about the common local *Z*-axis and also to move relative to one another, but in the vertical *Z*-sense only, i.e., $(p - s) \neq$ constant. As for the case with purely real coefficients, the roots are found from the two common points of intersection of the surfaces $A = B = 0$.

Location of the roots

To find the location of the roots in the *GH*-plane, a similar procedure to that described by Bardell (2012) is adopted. By definition, the roots occur when $y = 0$, implying that both $Re(y)$ and $Im(y)$ must simultaneously be zero. In other words, the location and nature of the roots will be defined where the two surfaces for $Re(y)$ $(\equiv A)$ and $Im(y)$ $(\equiv B)$ have a common intersection with a horizontal plane positioned at zero altitude. Analytically, this could be accomplished by solving Equations (5) and (6) simultaneously for G and H with both A and $B = 0$. However, this approach proves algebraically fairly intractable and will not be pursued further here, although it should nonetheless be mentioned that the resulting expressions for the roots x_1 at (G_1, H_1) and x_2 at (G_2, H_2) consist of the real and imaginary parts of Equation (2), as expected. It is also noted that in general $G_2 \neq G_1$ which is in contrast to the (conjugate) form of the roots (where $G_2 = G_1$) that was reported by Bardell (2012) when all the coefficients are real.

It is also stated, without proof, that if the roots are considered in the $G'H'$ axis system, which is centred at the combined surfaces' common local origin at (m, n) in the *GH* plane, then these roots are equi-pitched about this local origin and lie diametrically opposite each other on a circle of diameter:

$$D = \sqrt{(G_1 - G_2)^2 + (H_1 - H_2)^2} \tag{15}$$

In the special case when all the coefficients are real, $G_1 = G_2$ and hence Equation (15) reduces to:

$$D = (H_1 - H_2) = \frac{\sqrt{4a_R c_R - b_R^2}}{a_R} \tag{16}$$

which is recognised as the total distance along the H'-axis between a pair of conjugate roots.

Results and examples

In order to give some meaning to the concepts discussed above, attention will now be focused on the quadratic equation originally presented in Equation (3), which yields generally complex roots. In the three-dimensional surfaces that follow, the horizontal plane contains the $Re(x)$ $(\equiv G)$ and $Im(x)$ $(\equiv H)$

axes, thus forming the Argand plane, whilst the vertical axis represents either $Re(y)$ ($\equiv A$) or $Im(y)$ ($\equiv B$) depending on which surface is being investigated.

All the three-dimensional plots presented in this paper were constructed using *Mathcad* (2007), which is one of many VCE/QCE/HSC-approved computer algebra systems available to schools, and fully commensurate with the following ACARA (2009, Section 6.5.2) stated aim: "digital technologies can make previously inaccessible mathematics accessible, and enhance the potential for teachers to make mathematics interesting to more students".

Type I(a): Complex distinct roots

From Equation (3), the complex coefficients are: $a_R = 1$, $a_I = -1$; $b_R = -2$, $b_I = 6$; $c_R = 3$, $c_I = -2$. These data, when substituted in Equations (7d–7g) and (9d–9g) yield the surface parameters shown in Table 1; the roots follow from Equation (2) as: $x_1 = 0.414 + 0.419i$ and $x_2 = 3.586 - 2.419$i.

Table 1. The complex generalisation surface parameters for $y = (1 - i)x^2 + (-2 + 6i)x + (3 - 2i)$.

Surface A			**Surface B**		
Parameter	Value	Equation	Parameter	Value	Equation
Z_A	$\sqrt{2}X_A^2 - \sqrt{2}Y_A^2$	(8)	Z_B	$\sqrt{2}X_B^2 - \sqrt{2}Y_B^2$	(10)
m	2	(7d)	q	2	(9d)
n	–1	(7e)	r	-1	(9e)
p	4	(7f)	s	5	(9f)
β_A	$\pi/8$ or 22.5°	(7g)	β_B	$3\pi/8$ or 67.5°	(9g)

The surface A is constructed as described by Bardell (2012, pp. 8–9), and the following Figures 2 to 5 illustrate the key surface parameters summarised in Table 1. For clarity, the $G'H'$ axes are shown projected on the zero plane.

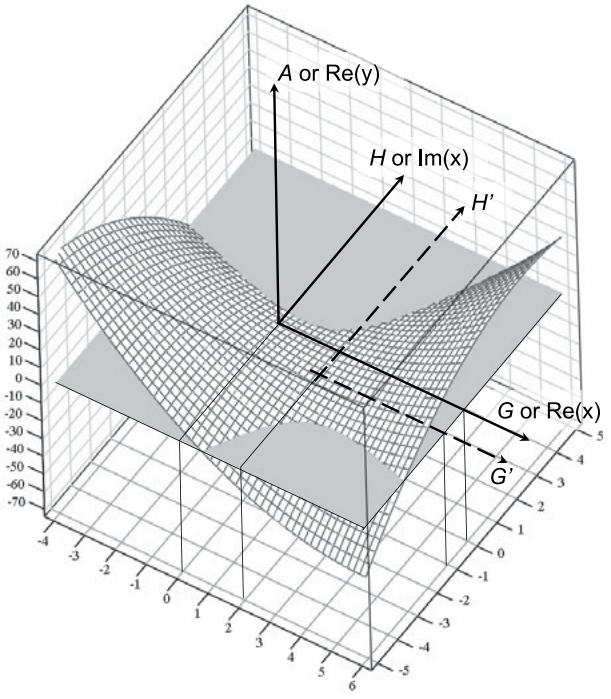

Figure 2. The surface A corresponding to the real part of the complex generalisation of $y = (1 - i)x^2 + (-2 + 6i)x + (3 - 2i)$.

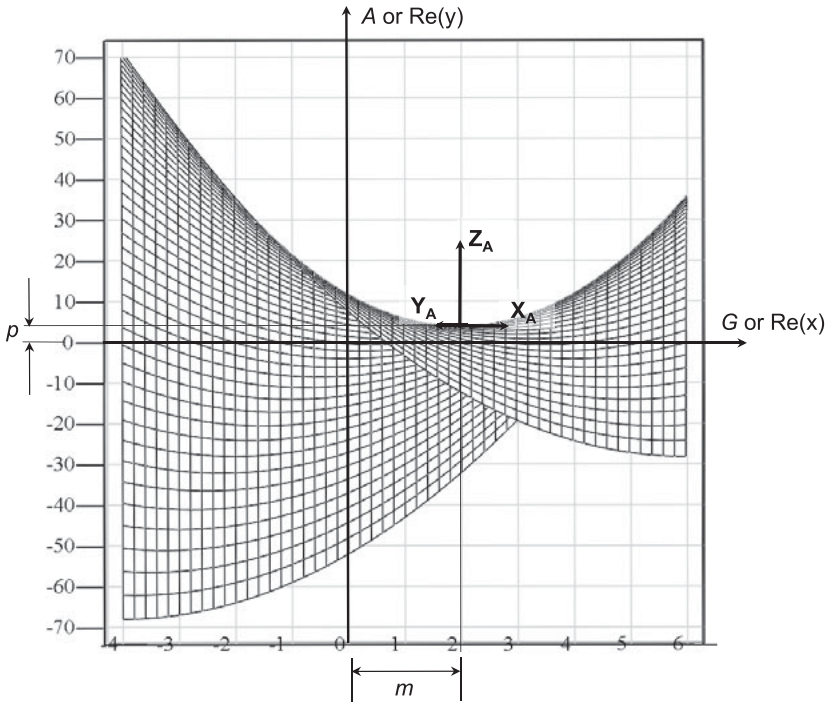

Figure 3. View on the GA plane of the surface A.

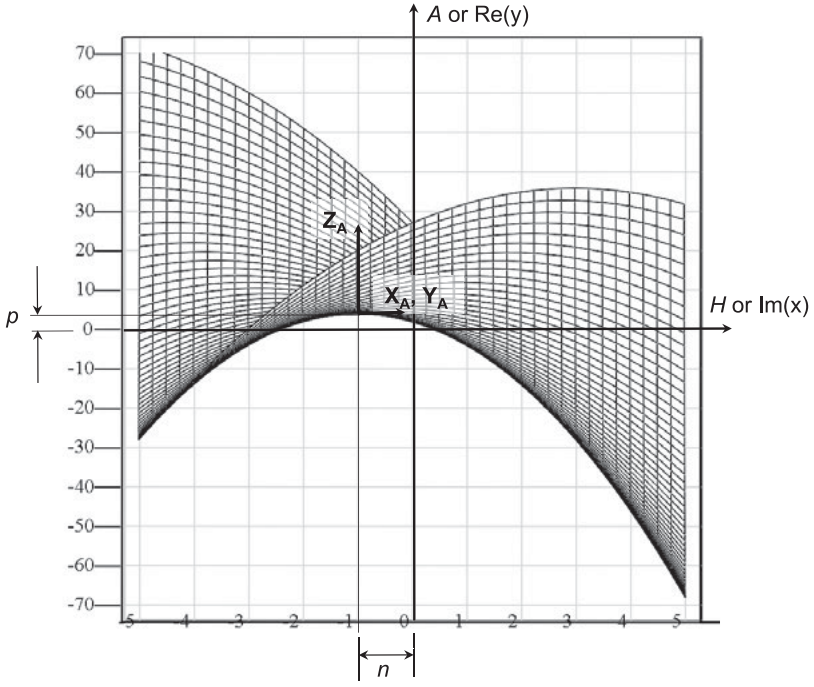

Figure 4. View on the HA plane of the surface A.

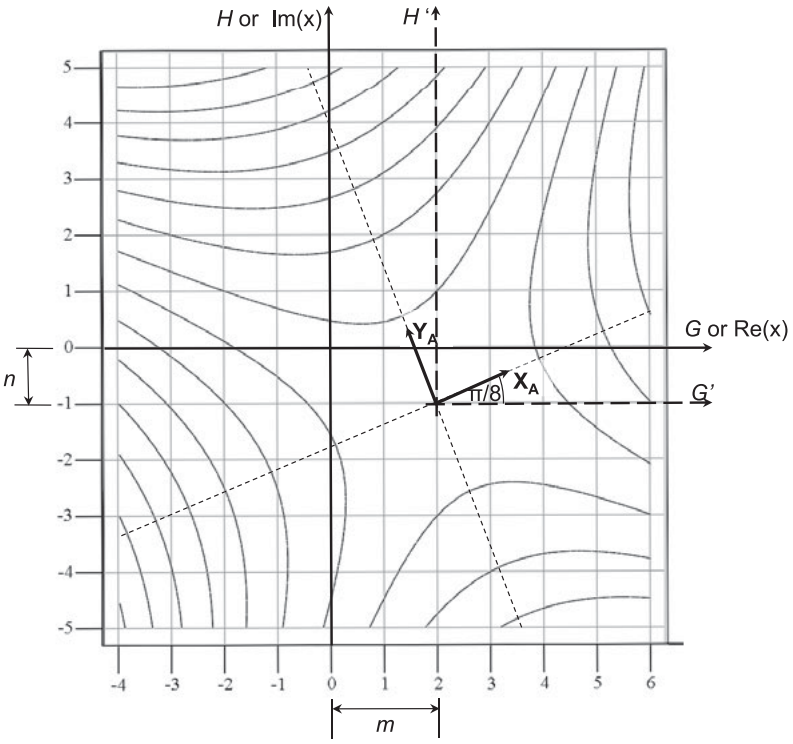

Figure 5. View on the GH plane of the surface A.

Figure 5 clearly shows the how the surface A is rotated by an angle $\pi/8$ counter-clockwise about its local origin at (m, n). Figures 6 to 9 are constructed for the surface B using the techniques described by Bardell (2012, pp. 8–9). These figures show a general quadric surface in contrast to the bi-linear (degenerate) case which resulted from purely real coefficients. Again, for clarity, the $G'H'$ axes are shown projected on the zero plane.

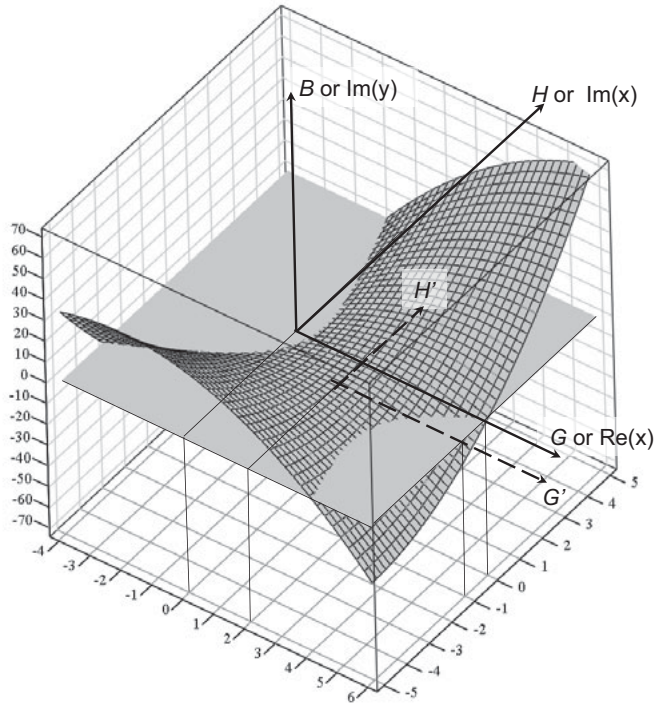

Figure 6. The surface B corresponding to the imaginary part of the complex generalization of $y = (1 - i)x^2 + (-2 + 6i)x + (3 - 2i)$.

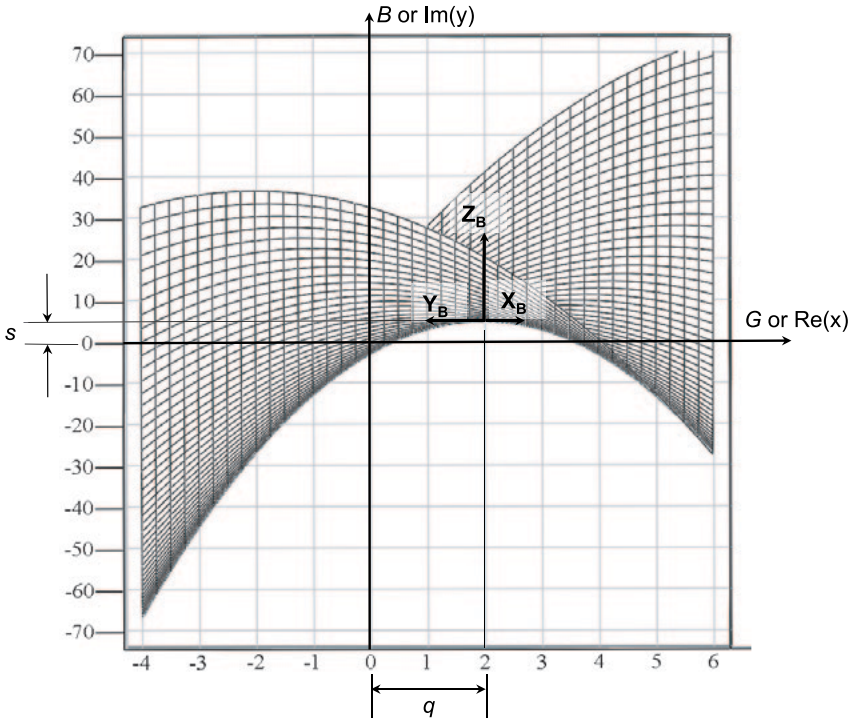

Figure 7. View on the GB plane of the surface B.

Figure 7 vividly shows $s \neq 0$ ($s = 5$ in this particular case) and Figure 8 shows $r \neq 0$ ($r = -1$ in this particular case). The surface B hence has more 'scope' to influence the location and nature of the roots than its real-coefficient counterpart investigated by Bardell (2012), in which both $s = 0$ and $r = 0$.

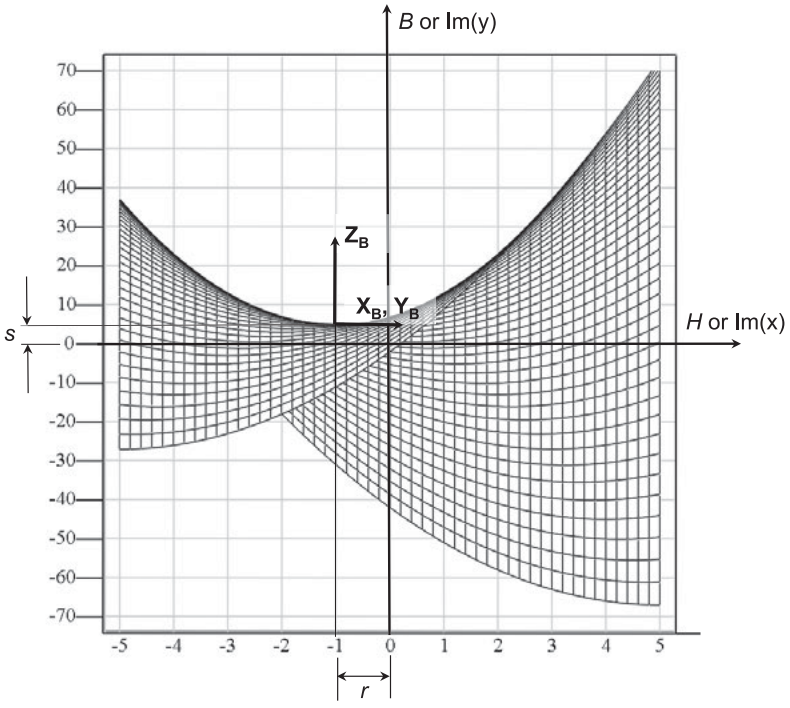

Figure 8. View on the HB plane of the surface B.

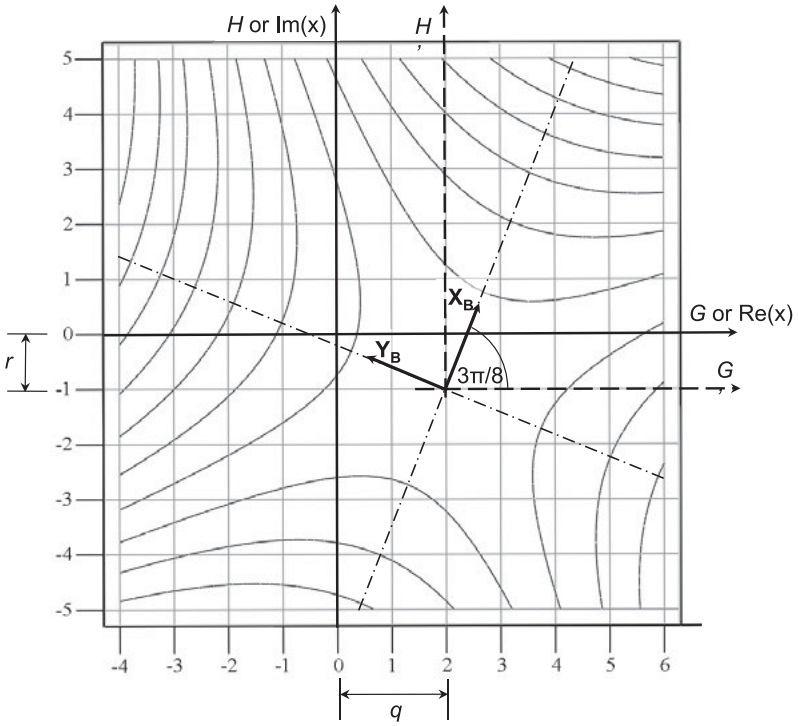

Figure 9. View on the GH plane of the surface B.

Figure 9 clearly shows how the surface B is rotated by an angle $3\pi/8$ counter-clockwise about its local origin at (q, r); superimposing Figures 9 and 5 shows how a constant angular difference of $\pi/4$ is always maintained between surface B and surface A as per Equation (14b).

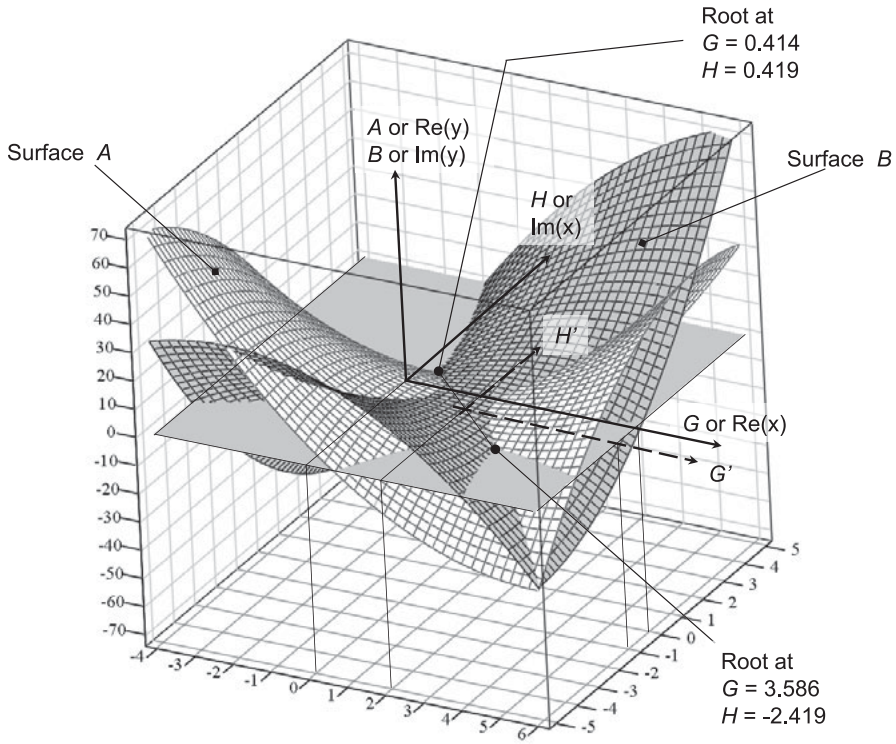

Figure 10. The distinct complex roots found at the common intersection of $A = B = 0$ from the complex generalization of $y = (1 - i)x^2 + (-2 + 6i)x + (3 - 2i)$.

As explained above, the complex roots are defined by the simultaneous satisfaction of Equations (5) and (6), namely $A = B = 0$, or $Re(y) = Im(y) = 0$. This is shown graphically in Figure 10 by the two points resulting from the intersection of the surfaces A and B with each other and with a horizontal plane positioned at zero altitude. These points are the two roots of the quadratic equation.

Figure 11 shows a view on the GH (Argand) plane from directly above. The location of the two roots at $G_1 = 0.414$ and $H_1 = 0.419$; i.e., $x_1 = 0.414 + 0.419i$ and at $G_2 = 3.586$ and $H_2 = -2.419$; i.e., $x_2 = 3.586 - 2.419i$ is clearly visible, being at the two unique points of intersection where $A = B = 0$. The location of the roots relative to the combined surfaces' common origin at $(2, -1)$ is $x_1' = -1.586 + 1.419i$ and $x_2' = 1.586 - 1.419i$. These roots are each of equal magnitude 2.128 units and located opposite each other on a circle of diameter 4.256 units.

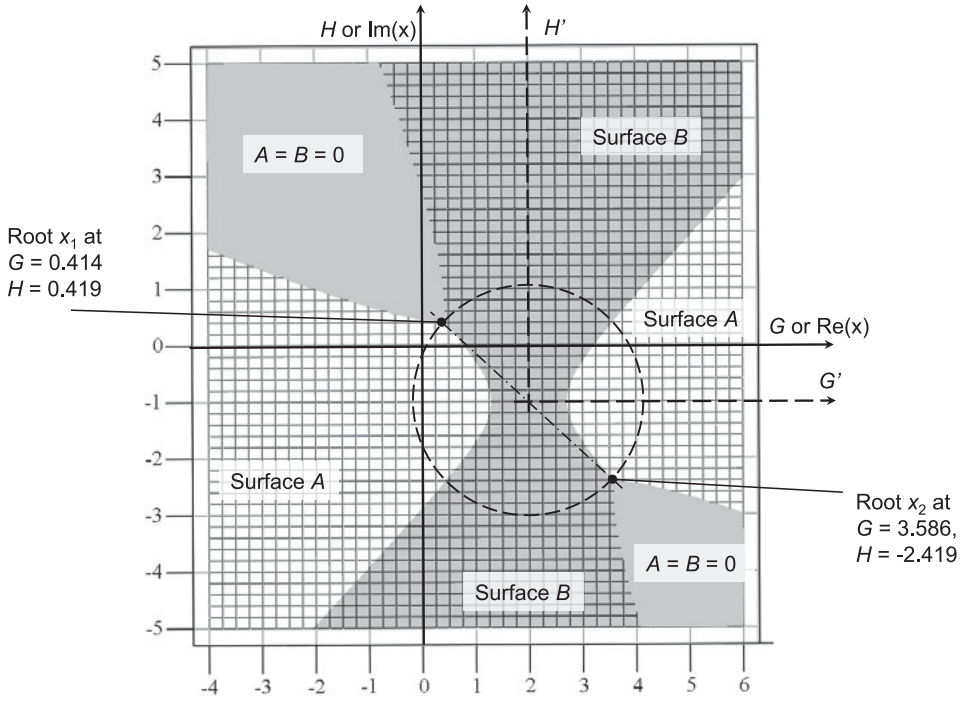

Figure 11. Plan view of the surfaces A and B showing the location of the generally complex roots of $y = (1 - i)x^2 + (-2 + 6i)x + (3 - 2i)$.

Finally, if a section is taken through both surfaces at $H = 0$, the traces of the 'cut' ends of surfaces A and B fully replicate the curves for $Re(y)$ and $Im(y)$ respectively shown in Figure 1. This vividly illustrates how the original x–y plane alone is merely a 'slice' of a much bigger picture, and is therefore very limited in the information it can convey for this type of problem.

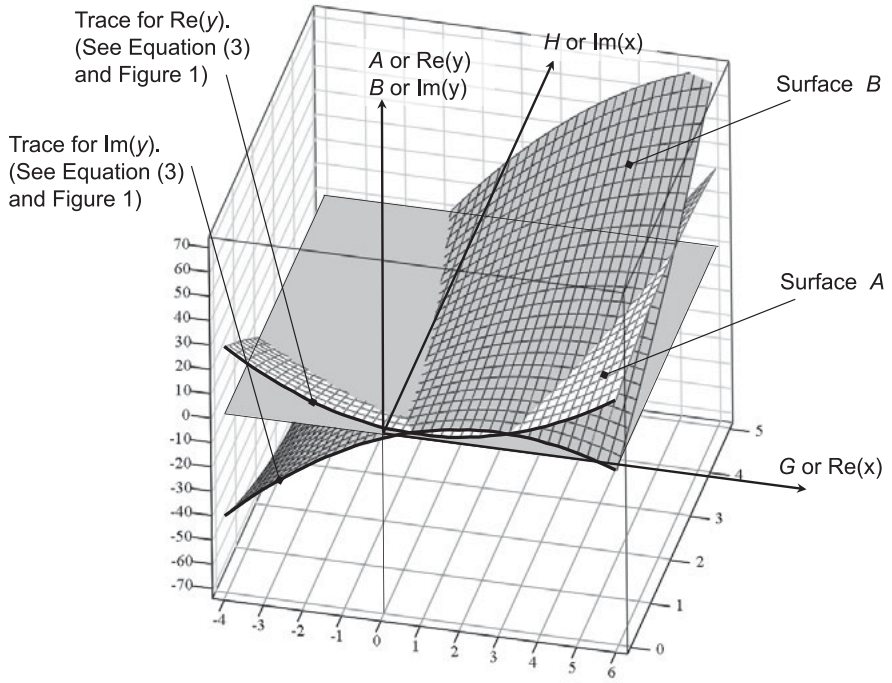

Figure 12. Section taken at H = 0 revealing the original traces of Re(y) and Im(y) from Equation (3) and Figure 1.

This completes the detailed review of a specific case in support of the methodology advanced in the section Theory. It is noted that for a given set of participating coefficients, generally complex roots (which includes real, imaginary, or a combination thereof) may be expected to occur. Some further examples are now given to illustrate the wide variety of root combinations that can exist for this type of quadratic equation with complex coefficients. These examples are intended to showcase some of the many different surface arrangements that can occur as the participating complex coefficients in a given equation are varied, and hence the plethora of roots that are possible.

Type I(b): Complex equal (repeated) roots

A pair of equal complex roots can only occur if $m \neq 0$ and $n \neq 0$ but $p = s = 0$ such that only a single point results from the intersection of $A = B = 0$. This is equivalent to ensuring the discriminant Δ in Equation (2) is zero. From a consideration of both the real and imaginary parts of the discriminant, this levies the following constraint on the complex coefficients:

$$b_R^2 - b_I^2 = 4(a_R c_R - a_I c_I) \text{ and } 2b_R b_I = 4(a_R c_I - a_I c_R) \qquad (17)$$

A suitable set of coefficients that satisfies Equation (17) is: $a_R = 4$, $a_I = 16/3$; $b_R = 8$, $b_I = 4$; $c_R = 3$, $c_I = 0$. These data yield $\Delta = 0$, $m = -0.6$, $n = 0.3$, $p = 0$, $s = 0$. The resulting equal (repeated) roots are $x_1, x_2 = -0.6 + 0.3i$. Note how these roots coincide with the common local origin (m, n) of both surfaces at altitude $p = s = 0$.

Type I(c): Complex conjugate roots

A pair of complex conjugate roots can occur, but only if:

- they fall on a line running parallel to the *H*-axis—to ensure the same real *G*-value; and
- the local origin of both surfaces is positioned at $n = 0$ in the GH-plane—to ensure equal and opposite imaginary $\pm H$-values.

McCarthy (n.d.) has proved that the complex coefficients must obey the criteria shown in Equation (18) to ensure conjugate roots:

$$b_R^2 - 4a_R c_R < 0 \text{ and } (a_R b_I - a_I b_R) = 0 \text{ and } (a_R c_I - a_I c_R) = 0 \qquad (18)$$

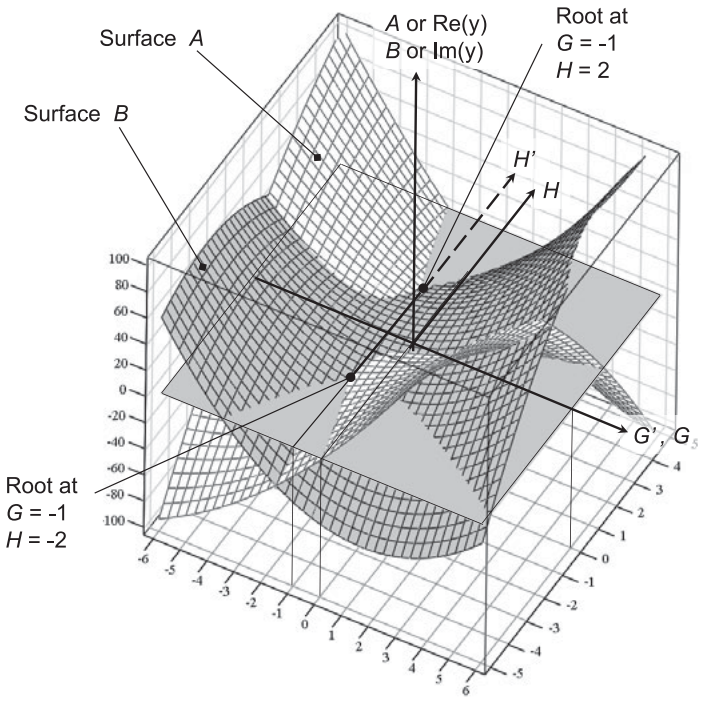

Figure 13. The complex conjugate roots found at the common intersection of A = B = 0 from the complex generalization of $y = (1 + 2i)x^2 + (2 + 4i)x + (5 + 10i)$.

McCarthy (n.d.) has shown further that if the complex coefficients are considered as vectors, then for complex conjugate roots to occur a, b, c must be collinear. A suitable set of coefficients that satisfies Equation (18) is: $a_R = 1$, $a_I = 2$; $b_R = 2$, $b_I = 4$; $c_R = 5$, $c_I = 10$. These data yield $\Delta = 48 - 64i$, $m = -1$, $n = 0$, $p = 4$, $s = 8$. From Equation (2) the resulting complex conjugate roots are $x_1 = -1 - 2i$, $x_2 = -1 + 2i$. These roots are shown in Figure 13. Each root is clearly equidistant from the local $G'H'$ origin at $(-1, 0)$. For clarity, the $G'H'$ axes are shown projected on the zero plane.

Hardy (2008, pp. 94–95) asserts that complex conjugate roots can exist only if all the coefficients are real. This is actually incorrect as will now be demonstrated. From the elementary theory of roots of a general quadratic equation, if $ax^2 + bx + c = 0$ has roots α, β, then by definition the sum of the roots $(\alpha + \beta) = -b/a$ and the product of the roots $\alpha\beta = c/a$. This condition

holds for coefficients that are either real or complex. If the roots form a complex conjugate pair, i.e., $\alpha = G + iH$ and $\beta = G - iH$, then clearly the sum of the roots $\alpha + \beta = 2G$ is real, and the product of the roots $\alpha\beta = G^2 + H^2$ is also real. This means that the sum and product quantities $-b/a$ and c/a in the original quadratic equation must also be real. This reasoning led Hardy to conclude that all the participating coefficients therefore had to be real for complex conjugate roots to result. However, this is not necessarily the case.[1] Only the ratios $-b/a$ and c/a must be real, but not the actual coefficients themselves. (In the current example, with complex coefficients, the ratios $-b/a = -2$ and $c/a = 5$ are most definitely real). The ratios are unique, but the actual values of a, b, c are not themselves uniquely determined. Now, it must also be noted that if the original equation with complex coefficients is divided through by the $(a_R + ia_I)$ term, $x^2 + 2x + 5 = 0$ results, and it could be argued that the complex coefficients given here reduce to a real coefficient example. However, the surface representations A and B that result from the two forms of the quadratic equation are quite different, indicating each equation is unique, even though the resulting roots turn out to be the same. This illustrates why rendering a quadratic equation monic, as Hardy does, masks certain important information, and shows that if only the roots are given, it is not possibly to reconstruct the original quadratic equation with complex coefficients unless the $(a_R + ia_I)$ term is known.

Type I(d): Purely imaginary roots

Purely imaginary roots can only occur if they lie somewhere on the line $G = 0$. McCarthy (n.d.) has proved that the criteria for this to occur are:

$$b_I^2 + 4a_Rc_R \geq 0 \text{ and } (a_Rb_I + a_Ib_R) = 0 \text{ and } (a_Rc_I - a_Ic_R) = 0 \qquad (19)$$

One possible set of coefficients that satisfies Equation (19) is: $a_R = 1$, $a_I = 1$; $b_R = -2$, $b_I = 2$; $c_R = 1$, $c_I = 1$. These data yield $\Delta = -16i$, $m = 0$, $n = -1$, $p = 2$, $s = 2$. The resulting roots are $x_1 = -2.414i$, $x_2 = 0.414i$. These roots are located equidistant from the local origin at $(0, -1)$ in the GH plane, as expected. McCarthy (n.d.) has also noted that if the complex coefficients are considered as vectors, then for purely imaginary roots to occur, $a \perp b$ and $a \parallel$ c, which is demonstrated by the numerical values used here.

Type II: Mixed roots—one complex root, one real root

A mixed root solution to Equation (1) can occur. The real root must lie somewhere along the G-axis (i.e, $H = 0$), but there is no restriction on the location of the complex root. No general criteria applicable to the coefficients have been reported that will guarantee this particular outcome. For clarity, the $G'H'$ axes are shown projected on the zero plane.

1 This conclusion is a direct conequence of Hardy (2008) making the term x^2 monic.

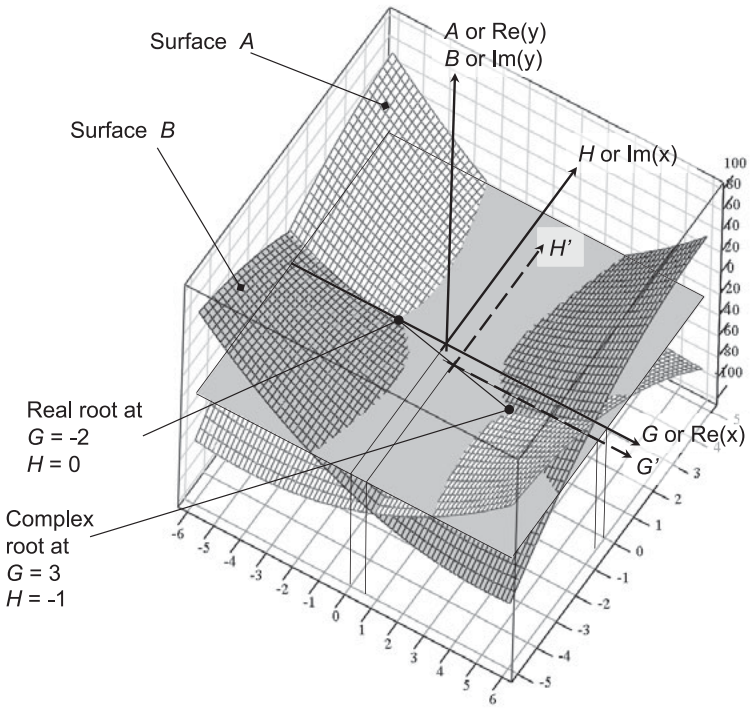

Figure 14. The mixed roots found at the common intersection of $A = B = 0$ from the complex generalisation of $y = (1 + i)x^2 - 2x + (-8 - 4i)$.

A suitable set of coefficients that will yield mixed roots is: $a_R = 1$, $a_I = 1$; $b_R = -2$, $b_I = 0$; $c_R = -8$, $c_I = -4$. These data yield $\Delta = 20 + 48i$, $m = 0.5$, $n = -0.5$, $p = -8.5$, $s = -3.5$. The resulting roots are $x_1 = -2$, $x_2 = 3 - i$ as shown in Figure 14. About their local $G'H'$ origin at $(0.5, -0.5)$ these roots become $-2.5 + 0.5i$ and $2.5 - 0.5i$, lying on a circle of diameter $\sqrt{26}$. A plot of this quadratic equation in the Cartesian x–y plane shows the $Re(y)$ and $Im(y)$ traces both crossing the x-axis at $x = -2$. This point locates the purely real root, but there is no further information available to indicate the whereabouts of the complex root (see Figure 15).

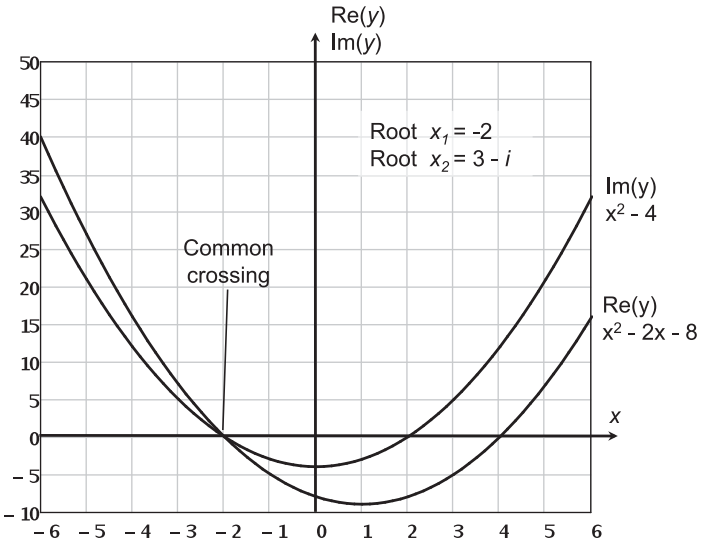

Figure 15. Plot of $y = (1 + i)x^2 - 2x + (-8 - 4i)$.

Note also that it is quite possible to have a mixed solution consisting of a purely real root and a purely imaginary root. The real root must lie somewhere along the *G*-axis (i.e, $H = 0$) and the imaginary root must lie somewhere along the *H*-axis (i.e, $G = 0$). Again, no general criteria applicable to the coefficients have been reported that will guarantee this particular outcome.

Type III(a): Real distinct roots

Roots that are real and distinct must both lie along the *G*-axis (i.e., $H = 0$).

McCarthy (n.d.) has proved that the complex coefficients required to produce a pair of purely real roots must obey the following criteria:

$$b_R^2 - 4a_Rc_R \geq 0 \text{ and } (a_Rb_I - a_Ib_R) = 0 \text{ and } (a_Rc_I - a_Ic_R) = 0 \qquad (20)$$

A set of coefficients that satisfies Equation (20) is: $a_R = 1$, $a_I = 0.5$; $b_R = 4$, $b_I = 2$; $c_R = -2$, $c_I = -1$. These data yield $\Delta = 18 + 24i$, $m = -2$, $n = 0$, $p = -6$, $s = -3$. The resulting real and distinct roots are $x_1 = -4.449$, $x_2 = 0.449$ as shown in Figure 16. Although both roots are real, the view of the combined surfaces presented here, and the manner of their intersection with each other and the zero plane, looks very different from that found from the analogous real-coefficient case (see Bardell, 2012). For clarity, the *G'H'* axes are shown projected on the zero plane.

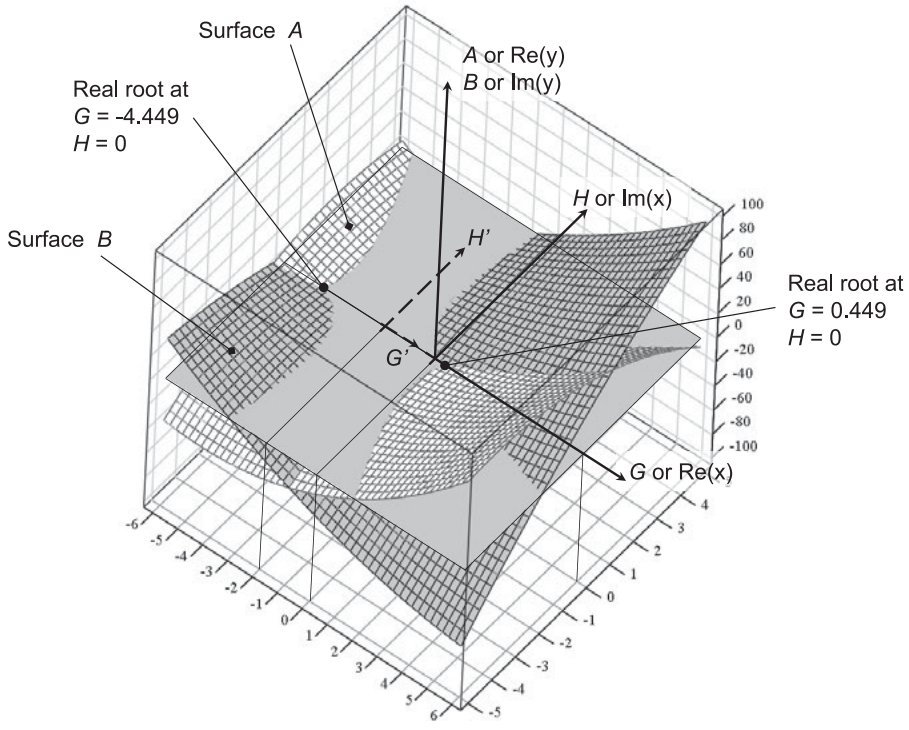

Figure 16. The real and distinct roots found at the common intersection of $A = B = 0$ from the complex generalisation of $y = (1 + i/2)x^2 + (4 + 2i)x + (-2 - i)$.

Again, contrary to popular belief, purely real roots can result from a quadratic equation with generally complex coefficients. McCarthy (n.d.) has shown further that if the complex coefficients are considered as vectors, then for real roots to occur a, b, c must be collinear, per the present example. This condition is the same as that applicable to finding complex conjugate roots, and only the additional constraint on the value of $b_R^2 - 4a_Rc_R$ dictates the final result. It is interesting to note that if $b_R^2 - 4a_Rc_R = 0$ then coincident real roots will result, these being the transition point between real and complex conjugate roots.

For the given example, following the argument presented for complex conjugate roots, a similar conclusion holds here. If the roots are purely real, i.e., $\alpha = G_1$ and $\beta = G_2$, then clearly the sum of the roots $\alpha + \beta = G_1 + G_2$ is real, and the product of the roots $\alpha\beta = G_1G_2$ is also real. This means that the sum and product quantities $-b/a$ and c/a must also be real which could lead one to conclude that all the participating coefficients therefore have to be real for real roots to result. However, only the ratios $-b/a$ and c/a must be real, but not the actual coefficients themselves. In the current example, $-b/a = 4$ and $c/a = -2$ (both real), yet the defining coefficients are themselves complex.

A plot of this quadratic equation in the Cartesian x–y plane ($H = 0$) shows the $Re(y)$ and $Im(y)$ traces have common intersections and cross the x-axis at $x_1 = -4.449$, $x_2 = 0.449$ which indicates the solution involves two real roots. It is noted the two roots are equi-spaced about the point (–2, 0) which is the common vertex of the curves represented by $Re(y)$ and $Im(y)$ in the x–y plane and of course the common vertex (m, n) of the surfaces A and B.

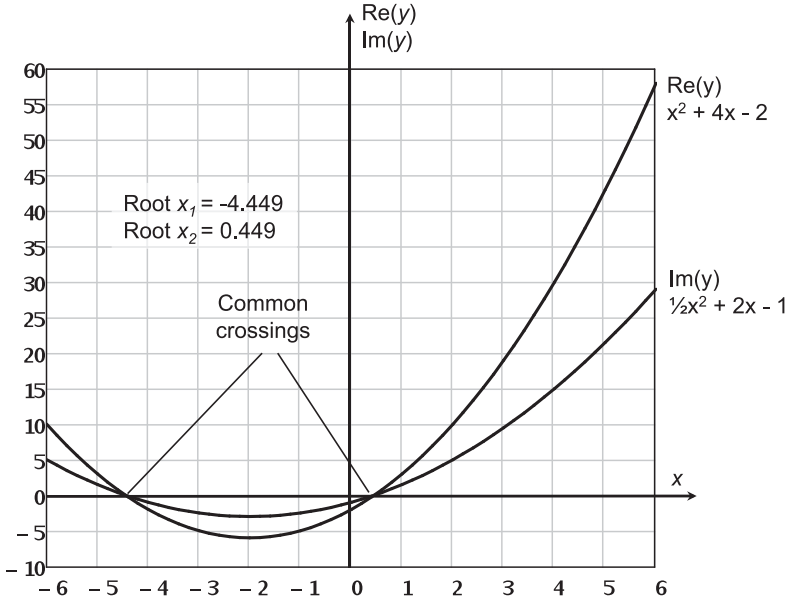

Figure 17. Plot of $y = (1 + i/2)x^2 + (4 + 2i)\ x + (-2 - i)$.

Type III(b): Real equal (repeated) roots

With reference to the complex repeated roots presented in section Type I(b), the same criterion applies here but with the additional constraint that now n or $r = 0$ (which implies $b_I a_R - a_I b_R = 0$ from Equation (7e)) to enforce a solution on the real GA plane. Hence the complex coefficients must now obey:

$$b_R^2 - b_I^2 = 4(a_R c_R - a_I c_I) \text{ and } 2b_R b_I = 4(a_R c_I - a_I c_R) \text{ and } (a_R b_I - a_I b_R) = 0 \quad (21)$$

Alternatively, from Section 3.5 above, the following [equivalent] condition also holds:

$$b_R^2 - 4a_R c_R = 0 \text{ and } (a_R b_I - a_I b_R) = 0 \text{ and } (a_R c_I - a_I c_R) = 0 \quad (22)$$

A set of coefficients that identically satisfies Equation (21) and Equation (22) is: $a_R = 1$, $a_I = 1/4$; $b_R = 4$, $b_I = 1$; $c_R = 4$, $c_I = 1$. These data yield $\Delta = 0$, $m = -2$, $n = 0$, $p = 0$, $s = 0$. The local origin of both surfaces lies on the zero plane at $GH = (-2, 0)$ and is itself the single point that results from the intersection of $A = B = 0$. Hence the resulting repeated real roots are $x_1 = x_2 = -2$, coincident with the local origin.

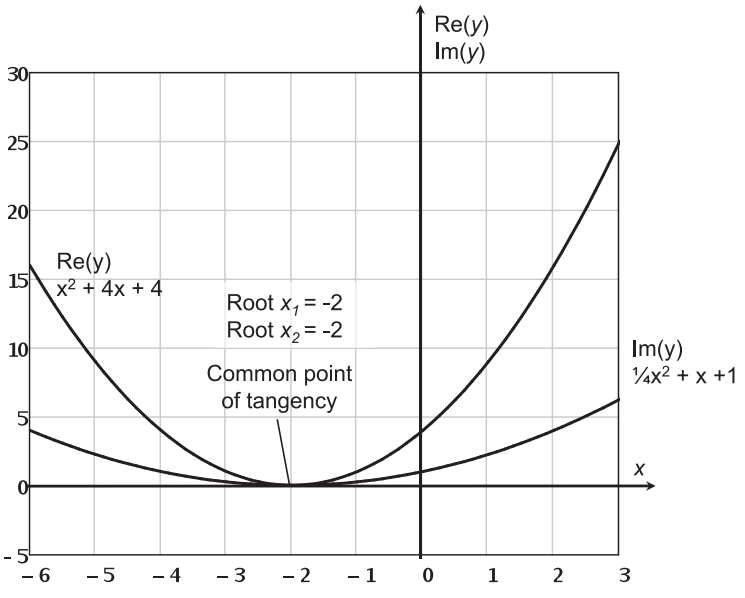

Figure 18. Plot of $y = (1 + i/4)x^2 + (4 + i)x + (4 + i)$.

Figure 18 shows the traces of the $Re(y)$ and $Im(y)$ parts of the quadratic equation in just the Cartesian x–y plane ($H = 0$). Both curves have a single common point of intersection that is also tangential with the x-axis at $x = -2$. This point indicates the location of a repeated real root.

Conclusions

A quadratic equation with generally complex coefficients can yield any possible combination of roots. This is in complete contrast to the real-coefficient counterpart studied by Bardell (2012). For a given set of complex coefficients it is not easy to predict what type and combination of roots will result—to this end some general criteria have been either quoted from McCarthy (n.d.) and verified, or developed from the graphical considerations presented herein.

This paper has shown that the complex generalisation of a quadratic equation may easily be extended to accommodate the case with complex coefficients. The roots are still found from the intersection of the hyperbolic paraboloid surfaces A and B, representing the real and imaginary parts of the generalisation respectively, with a plane at zero altitude, as first described by Bardell (2012). Many similarities between the two types are evident, although when the coefficients are generally complex any possible combination of the roots may occur. This is primarily due to both three-dimensional surfaces exhibiting a greater freedom of orientation and elevation compared with their real-coefficient counterparts and thus more varied opportunities to intersect each other and the zero plane. A fuller understanding of this, and other phenomena, has been facilitated by the visualisation techniques presented in this paper. It has further been shown that the roots are always spaced equi-distant from the common local origin of the real and imaginary defining surfaces, and only under special circumstances do complex conjugate roots now result. Attempts to plot a quadratic equation with complex coefficients in only the Cartesian x–y plane fail to reveal any useful information about the location and nature of the roots unless they happen to contain a purely real part, in which case the curves representing $Re(y)$ and $Im(y)$ must both coincide at the point where they intersect the x-axis.

Finally, it should be mentioned that teachers can use programs such as *Mathcad* (2007) to show students how hyperbolic paraboloid surface functions, such as A and B described herein, can be easily plotted, zoomed, rotated, etc. The subject matter presented in this paper could easily form the basis of a classroom-based learning exercise in three-dimensional graphics using computer algebra systems that would amply satisfy the ACARA (2009, Section 6.5.1) stated aim, namely, that "digital technologies allow new approaches to explaining and presenting mathematics".

References

Australian Curriculum, Assessment and Reporting Authority [ACARA]. (n.d.) *Senior Secondary Curriculum – Specialist Mathematics Curriculum. Unit 3*. Retrieved from http://www.australiancurriculum.edu.au/SeniorSecondary/mathematics/specialist-mathematics/Curriculum/SeniorSecondary#page=3

Australian Curriculum, Assessment and Reporting Authority [ACARA]. (n.d.) *Senior Secondary Curriculum – Specialist Mathematics Curriculum. Rationale*. Retrieved from http://www.australiancurriculum.edu.au/SeniorSecondary/mathematics/specialist-mathematics/RationaleAims

Australian Curriculum, Assessment and Reporting Authority [ACARA]. (2009). *Shape of the Australian Curriculum: Mathematics*. Retrieved from: http://www.acara.edu.au/verve/_resources/Australian_Curriculum_-_Maths.pdf

Bardell, N. S. (2012). Visualizing the roots of quadratic equations with real coefficients. *Australian Senior Mathematics Journal, 26*(2), 6–20.

Board of Studies NSW. (1997). *HSC mathematics extension in NSW*. Retrieved from http://www.boardofstudies.nsw.edu.au/syllabus_hsc/pdf_doc/maths4u_syl.pdf

Hardy, G. H. (2008). *A course of pure mathematics centenary edition* (10th ed.). Cambridge, UK: Cambridge University Press.

McCarthy, P. J. (n.d.). *Discriminant for the quadratic equation with complex coefficients*. Retrieved from http://pauljmccarthy.us/

Parametric Technology Corporation (2007). *Mathcad 14.0*.

Queensland Studies Authority. (2009). *Queensland Mathematics C senior syllabus*. Retrieved from http://www.qsa.qld.edu.au/yrs11_12/subjects/maths_c/syllabus.pdf

Victorian Curriculum and Assessment Authority [VCAA]. (2010). *VCE Specialist Mathematics*. Retrieved from http://www.vcaa.vic.edu.au/vce/studies/mathematics/mathsstd.pdf